



LAWRENCE
LIVERMORE
NATIONAL
LABORATORY

Niobium Oxide Film Deposition Using a High-Density Plasma Source

R. Chow, M.A. Schmidt, A.W. Coombs, J.
Anguita, M.J. Thwaites

March 1, 2006

49th Annual SVC Technical Conference
Washington, DC, United States
April 22, 2006 through April 27, 2006

Disclaimer

This document was prepared as an account of work sponsored by an agency of the United States Government. Neither the United States Government nor the University of California nor any of their employees, makes any warranty, express or implied, or assumes any legal liability or responsibility for the accuracy, completeness, or usefulness of any information, apparatus, product, or process disclosed, or represents that its use would not infringe privately owned rights. Reference herein to any specific commercial product, process, or service by trade name, trademark, manufacturer, or otherwise, does not necessarily constitute or imply its endorsement, recommendation, or favoring by the United States Government or the University of California. The views and opinions of authors expressed herein do not necessarily state or reflect those of the United States Government or the University of California, and shall not be used for advertising or product endorsement purposes.

Niobium Oxide Film Deposition Using a High-Density Plasma Source

R. Chow, M.A. Schmidt, A.W. Coombs
Lawrence Livermore National Laboratory, Livermore, CA, USA

J. Anguita, M.J. Thwaites
Plasma Quest Limited, Hampshire, England

Abstract

Niobium oxide was deposited reactively using a new type of high-density plasma sputter source. The plasma beam used for sputtering is generated remotely and its path to the target defined by the orthogonal locations of two electromagnets: one at the orifice of the plasma tube and the other just beneath the target plane. To accommodate very large batches of substrates, the trade-off between load capacity and deposition rates was evaluated. The effect on deposition rate was determined by moving the plasma source away from the target in one direction and by moving the target assembly away in an orthogonal direction. A simple methodology was used to reestablish the reactive deposition rate and oxide quality even when large changes were made to the chamber geometry. Deposition parameters were established to produce nonabsorbing niobium oxide films of about 100- and 350-nm thicknesses. The quality of the niobium oxide films was studied spectroscopically, ellipsometrically, and stoichiometrically.

Key Words: Deposition Rate; Reactive Sputtering; Optical Coating

Introduction

High-quality, refractory metal, oxide coatings are required in a variety of applications such as high-power laser optics [1], microelectronic insulating layers [2], nanodevice structures [3], electro-optic multilayers [4], and sensors [5]. The control of microscopic defects is paramount within these oxides in order for them to function in critical applications where, at times, failure may lead to catastrophic damage. The metal oxides can be deposited by a variety of coating techniques. The physical vapor deposition process that is discussed in this paper is reactive sputter deposition with the expressed purpose of characterizing a particular refractory metal oxide.

A new high-density plasma (HDP) source is available commercially for sputter deposition. A description of the HDP and its configuration has been reported [6,7]. One advantage of this source is that the high plasma density lends itself to higher deposition rates for reactive sputtering, an important parameter in the production of metal oxides. Another, more subtle, advantage is the ability to independently control the ion density and the target bias voltage. This adds another means to control oxide properties that are not available in typical magnetron sputter sources. The source can be fitted to various chambers sized from 40 x 40 x 50 cm to very large web coaters. However, there are some chamber configurations designed for high throughput or with other deposition techniques that preclude easy installation of the HDP source in a configuration optimized for high deposition rates. The purpose of this study was to determine the deposition rate dependency of the HDP source on deviations from the optimal geometric configuration. The study was performed during the reactive deposition of Nb

oxide. The quality of the Nb oxide films was characterized spectroscopically, ellipsometrically, and stoichiometrically.

Experimental Setup

The experiments were done on a stainless steel vacuum chamber that had cryo- and turbo-vacuum pumps. The chamber size was 60 x 120 x 85 cm (width x depth x height). To maximize the number of runs in a short time, the base pressure of the vacuum system before each test was only 3.3 mPa. Figure 1 is a sketch of the configuration of the high-density plasma source, target and substrate planet locations. The plasma source was mounted on the left sidewall of the chamber as one faces the access door. The target is 22.86 cm to the right of the plasma source orifice, and 7.62 cm below the centerline of the plasma source. For the reactive sputter deposition of Nb oxide, the substrate planet was a single axis rotation, 10.16 cm off-center from the target, and 12.06 cm above the target plane. The plasma orifice used in this study had an inner diameter of 15.24 cm. The 99.95% pure Nb metal target was 10.16 cm in diameter.

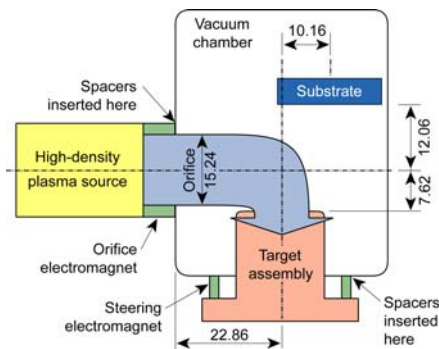


Figure 1. High-density plasma source geometry for reactive sputter deposition.

There are two electromagnets, one positioned at the orifice of the plasma source and the other below the target. The latter is called the steering electromagnet. Both electromagnets enhance the electron mean free path in the space between the plasma orifice and the target. When the RF power is applied to the coils around the plasma source, the Ar atoms are ionized. The current to the orifice electromagnet was kept constant at 148 A, while the current to the steering electromagnet was adjusted to steer the HDP beam onto the target. The following parameters were also kept constant for the tests results presented in this paper. The Ar flow was 140 sccm and injected near the target plane to minimize target poisoning. The RF power was set at 4 KW. The target was biased at -1.0 KVdc. This potential accelerates the Ar^+ across the dark space sheath to sputter the target material.

To increase the distance between the plasma source orifice and the centerline of the target, spacers were inserted between the plasma source and the vacuum chamber, while keeping the target at a constant height. Similarly, the target and steering magnet unit were lowered with spacers, while keeping the plasma source mounted against the chamber sidewall.

Thin films of Nb oxide were deposited reactively onto Si(100) single-crystal, microscope glass slide and Kapton[®] film substrates. Thickness profiling, optical spectroscopy and stress analysis were

performed, respectively, on these substrates. These films had thicknesses of about 300 to 400 nm. Niobium oxide films deposited to about 100-nm thickness on the Si substrates were used for analysis by X-ray photoelectron spectroscopy and variable-angle spectroscopic ellipsometry. The O₂ was injected near the substrate plane. The O₂ flow was adjusted to maintain a constant ratio of 2.66 O₂ molecules (injected) to Nb (sputtered) atoms. The O₂ concentration was determined with the flow rate of 60 sccm under the constant experimental conditions and setup shown in Figure 1. The sputtered Nb concentration was determined from the target current and adjusted by 0.90 for the sputter yield of Nb by 1 KeV Ar⁺ [8].

The transmittance of the Nb oxide films was performed from 1100 to 300 nm, using an Avantes AvaSpec 2048 model UV-VIS-nIR spectrophotometer. The spectral contributions of the microscope slide were accounted for by calibrating the spectrophotometer background noise with an uncoated glass slide inserted in the beam path. The coated glass substrates were then measured in transmittance to reveal the spectral effects of the coating. The refractive indices of the 360-nm Nb oxide films were determined from these transmittance scans, using an approach after Manifacier et al [9].

Variable-angle spectroscopic ellipsometry was performed using a Woollam V-VASE[®] HS-190 ellipsometer system. The angles used were 65°, 70°, and 75°. The wavelengths used in spectroscopy were from 193 to 1770 nm. A Nb oxide/native Si oxide/Si substrate stack was set up in the analysis application, where the optical properties of the silicon single crystal and its native oxide that were supplied with the instrument were used. A Tauc-Lorentz oscillator model was used to fit the ellipsometry data for the extinction coefficients, and then the Kramers-Kronig relationship was used to derive the refractive indices [10].

Results and Discussion

Deposition Rate

The geometry and distances described in Figure 1 do not place the orifice of the plasma source at the optimal distance from the centerline of the target to obtain the highest deposition rate. In any case, as the orifice of the plasma source was pulled away from the centerline of the target, the deposition rate decreased. The deposition rate was determined from the time of deposition and the film thickness, as measured by contact profilometry over a stepped area of the coating. The rate change is more sensitive nearer to the optimal distance, a 6.1- compared to a 3.8-%/cm rate change. The average decrease is 4.9% of the rate/cm in the distance regime of 5 to 22 cm from the optimal distance. The rate dependency of moving the source in the horizontal direction is shown in Figure 2a.

The plasma source was returned to its position on the wall of the vacuum chamber, and then the target assembly was moved vertically in two sequential steps. This lowering of the target assembly increased the distance between the centerline of the plasma source and the face of the target. As the target assembly is lowered, the throw distance between the target and substrate plane increases as well. The deposition rates at constant throw distance were calculated from the change in the target current at constant Ar flow, target bias, RF power, and current to the electromagnet at the orifice. The target current is a measure of the Ar⁺ concentration available for sputtering and, therefore, the deposition rate if the throw distance is kept constant. In this series of tests, the target assembly did pass through the

optimal position for a high deposition rate as shown by the peak in Figure 2b. The absolute rate changes of moving closer and further from the optimal distance was 6.4 and 4.6 %/cm, respectively.

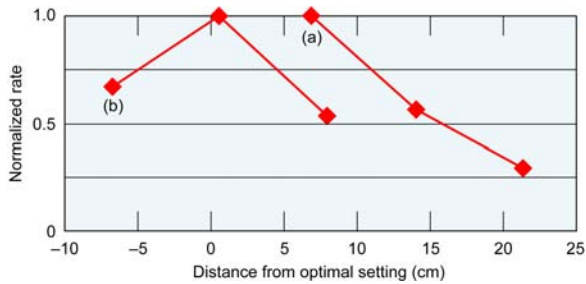


Figure 2. (a) Moving the plasma source further away from the optimal distance decreases the deposition rate monotonically. The average slope is -4.9% /cm. (b) Moving the target away from the optimal distance decreases the deposition rate at about -5% /cm. Calculated deposition rates were done for a constant throw distance between the substrate and target planes.

The distances traversed by moving the target assembly are of the same range as moving the plasma source. The dependence of the rate changes are also of the same order of magnitude, even though the target assembly did pass through the high rate configuration. In contrast, the data in Figure 2a indicate that larger rate changes should be expected as one moves the plasma source closer towards a high deposition rate configuration (i.e., closer to the target centerline). The deposition rate of the HDP source may be more sensitive to the distance between the plasma source and target centerline than the distance between the target plane and plasma source centerline. In setting up the HDP source in larger chambers, the least sensitive direction upon deposition rate is between the target and the plasma source centerline. There are other means to compensate for non-optimal source and target configurations to regain higher deposition rates. The methods basically are to make more efficient use of or to increase the concentration of available Ar^+ . Such methods may be to increase the plasma density at the target plane by increasing the size of the plasma source, the target diameter, RF power to the source, or even adjusting the magnetic field strengths between the source and target by designing electromagnets with higher current capacity.

Niobium Oxide Properties

The oxide phase was confirmed to be Nb_2O_5 by X-ray photoelectron spectroscopy. Figure 3 shows the high-resolution scans of the Nb_2O_5 film at four locations along the 50-mm radius of a coated Si substrate. The curves were adjusted for surface charging, based on the energy shift from the C 1s peak. In each scan, the Nb 3d5/2 peak is observed near 207.5 eV, indicative of Nb_2O_5 . If the NbO phase had formed, the 3d5/2 peaks would have been observed at 203.8 eV [11].

Transmittance scans of the Nb oxide films were performed for every change of the plasma source geometry. A typical transmittance scan from one of the Nb oxide thin films is given in Figure 4. The transmittance minima and maxima are due to constructive interference between multiple orders of quarter wave optical thicknesses. All the scans show high transparency from 1100 down to about 400 nm. Even though there were large changes to the physical layout of the plasma source and target positions, transparent oxide films were consistently achieved simply by adjusting the O_2 flow to

maintain a constant ratio of O₂ to metal. The deposition times were varied to keep consistent film thicknesses.

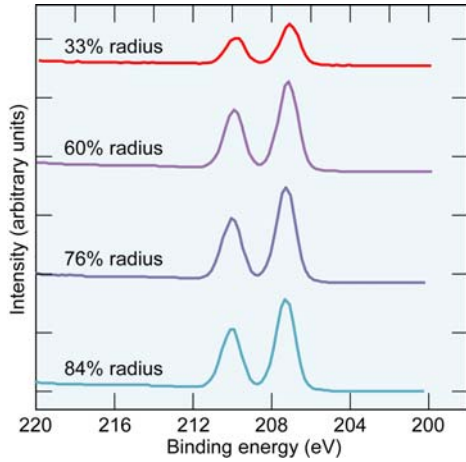


Figure 3. Binding energy of the Nb 3d_{5/2} and 3d_{3/2} electrons from high resolution X-ray photoelectron spectroscopy. The 3d_{5/2} peak at 207 eV indicates formation of the Nb₂O₅ phase.

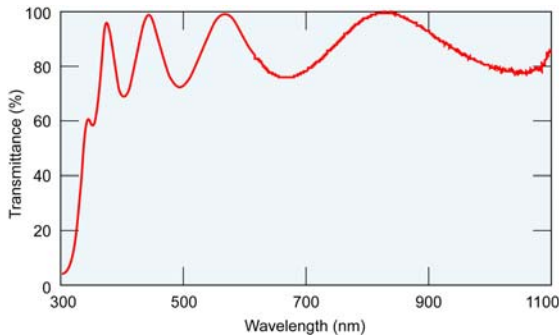


Figure 4. Transmittance scan of a 360-nm-thick Nb₂O₅ coating on a glass substrate.

The dispersion curve was obtained from modeling the results from the variable angle spectroscopic ellipsometer scan from 193 to 1800 nm on films 100 nm thick. The Cauchy equation representing the dispersion curve from 590 to 1770 nm is

$$n = 2.217 + 0.0701/\lambda^2 - 0.0058/\lambda^4 \quad \text{Eqn. [1]}$$

where λ is the wavelength in microns; and the errors for the first, second, and third terms are ± 0.004 , ± 0.005 , and ± 0.00123 , respectively. These and the refractive indices determined from the 360-nm-thick Nb oxide coatings on glass slides are plotted in Figure 5. The two dispersion curves overlay each other very well, indicative that the thicker films are also Nb₂O₅.

The Nb oxide dispersion curves from the HDP source are compared to those deposited by DC reactive magnetron sputtering [12,13] and electron-beam evaporation [14] methods in Figure 5. Bulk [15] and ion-beam sputtered [16] refractive indices at about 640 nm are also plotted for reference. The HDP-deposited Nb₂O₅ films have dispersion curves with higher refractive indices than the ion-beam

sputtered, DC magnetron sputtered, and e-beam deposited films. Refs. 12 and 13 determined that their as-deposited Nb oxide films were about 87% of bulk density by using the Clausius-Mossotti packing density relationship [17]

$$P = (n_f^2 - 1) (n_b^2 + 2) / (n_f^2 + 2) / (n_b^2 - 1) \quad \text{Eqn. [2]}$$

and about 95% of bulk density by gravimetry and X-ray reflectometry, respectively. Applying Equation 2 to the HDP-deposited Nb₂O₅ films, the as-deposited density is 98% of bulk, where n_f and n_b are 2.35 and 2.40, respectively, at 650 nm. Another possible cause for higher refractive indices might be the presence of metal-rich suboxides, but the XPS analysis did not indicate such a presence in the oxides deposited by the HDP source. These Nb₂O₅ films deposited by a HDP source have a near-bulk density.

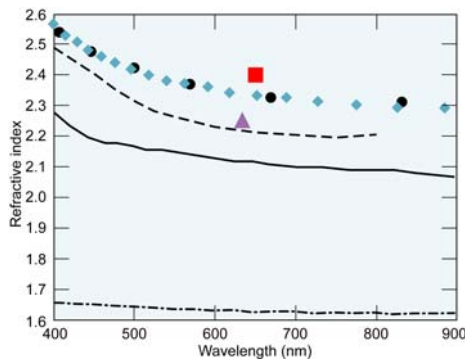


Figure 5. Dispersion curves of Nb oxides from the 100- and 360-nm-thick coatings by a HDP source, as determined from transmittance minima and maxima (o) and from variable-angle spectroscopic ellipsometry (◆); DC magnetron sources that were as-deposited 87% (—) and 95% (----) of bulk density; and e-beam deposited (· - ·). Refractive indices from bulk- (■) and ion-beam deposited (▲) Nb oxides are given at 650 and 633 nm, respectively.

The refractive indices and extinction coefficients at the shorter wavelengths were determined from the multiwavelength ellipsometric data and are shown in Figure 6.

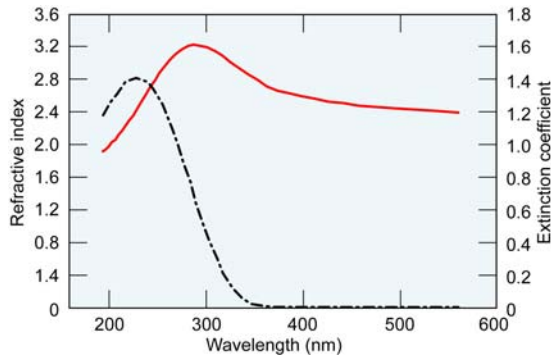


Figure 6. Refractive indices (—) and extinction coefficients (---) of Nb₂O₅ in the short-wavelength regime.

The compressive film stress was determined to be 517.3 MPa from the Stoney equation [18]

$$\sigma = E_s t_s^2 / (6 r (1 - \nu) t_f) \quad \text{Eqn. [3]}$$

where $E_s = 2.5$ GPa, Young's Modulus for Kapton[®] film; $t_s = 45$ microns, the substrate thickness; $r = 12.5$ mm, the radius of curvature; $\nu = 0.63$, Poisson's ratio for Kapton[®] film; and $t_f = 360$ nm, the film thickness. This stress value is comparable to that reported for ion-beam-deposited Nb oxide of -375 to -460 MPa [16]. A much lower stress is reported for DC magnetron-deposited Nb oxide of -120 MPa [13]. The use of the process [7] or reactive [19] gas pressures during deposition has been shown to change the film stress from compression to tension. This will be part of the future process development using the HDP source for reactive sputtering.

Summary

A simple methodology was used to obtain high-quality Nb₂O₅ even as large changes were made to the setup of the high-density plasma deposition system. This indicates robustness in manufacturing processes using this new sputtering technology.

The deposition rate characteristics of a high-density plasma source were evaluated. The deposition rates decrease about 5 %/cm as the plasma source or target assembly is moved away from a high-rate geometry. However, the deposition rate may be more sensitive to distance changes between orifice of the plasma tube and the centerline of the target.

Reactive sputtering with a HDP source of metal Nb in the presence of an O₂ partial pressure produced stoichiometric Nb₂O₅. The refractive indices from 193 to 1770 nm and extinction coefficients from 193 to 400 nm were determined for as-deposited Nb₂O₅ by transmittance and ellipsometry. These Nb₂O₅ films are 98% of bulk density and have compressive stresses comparable to that of ion-beam-deposited Nb oxide thin films.

Auspices and Acknowledgements

This work was performed under the auspices of the U.S. Department of Energy by University of California, Lawrence Livermore National Laboratory under Contract W-7405-Eng-48.

The authors would like to thank Art J. Nelson of LLNL, Cheryl L. Evans of LLNL, and Neha Singh of J.A. Woollam Co., Inc. for surface analysis of the films.

References

1. M. R. Kozlowski, R. Chow, I. M. Thomas, "Optical coatings for high power lasers," *Handbook of Laser Science and Technology*, 767, CRC Press, Inc., Boca Raton, 1995.
2. S.J. Kim, B.J. Cho, M.B. Yu, M.F. Li, Y.Z. Xiong, C. Zhu, Chin A., D.L. Kwong, "Metal-insulator-metal RF bypass capacitor using niobium oxide with HfO₂ Al₂O₃ barriers," *IEEE Electron Device Letters*, 26 (9), 625, 2005.
3. F. Richter, H. Kuper, P. Schlott, T. Gessner, C. Kaufmann, "Optical properties and mechanical stresses in SiO₂-Nb₂O₅ multilayers," *Thin Solid Films*, 389 (1-2), 278, June 2001.
4. Z.W. Fu, J.J. Kong, Q.Z. Qin, "Electrochemical and electrochromic properties of niobium oxide thin films fabricated by pulsed laser deposition," *J Electrochem Soc*, 146 (10), 3914, 1999.

5. S. Murray, M. Trudeau, D.M. Antonelli, "Synthesis and magnetic tuning in superparamagnetic cobaltocene-mesoporous niobium oxide composites," *Advanced Materials*, 12 (18), 1339, Sept. 2000.
6. M. Vopsaroiu, M.J. Thwaites, S. Rand, P.J. Grundy, K. O'Grady, "Novel sputtering technology for grain-size control," *IEEE Transaction on Magnetics*, 40 (4), 2443, 2004.
7. P.J. Hockley, M.J. Thwaites, G. Dion, "High density plasma deposition," *SVC 48th Annual Technical Conference Proceedings*, Society of Vacuum Coaters, 2005.
8. D. L. Smith, *Thin Film Deposition*, Appendix C, McGraw-Hill Inc., NY, 1995.
9. J.C. Manificier, J. Gasiot, J.P. Fillard, "A simple method for the determination of the optical constants n , k and the thickness of a weakly absorbing thin film," *J Phy E*, 9, 1002, 1976.
10. J.A. Woollam Co., Inc., *Guide to using WASE32TM*, WexTech, New York, 269, 1995.
11. J.F. Moulder, W.F. Stickles, P.E. Sobol, K.D. Bomben, *Handbook of X-ray Photoelectron Spectroscopy*, 111, J. Chastin and R.C. King Jr., Eds., Physical Electronics, Inc., Eden Prairie, MN, 1995.
12. S. Venkataraj, R. Drese, O. Kappertz, R. Jayavel, M. Wuttig, "Characterization of niobium oxide films prepared by reactive DC magnetron sputtering," *Phys Stat Sol A*, 188 (3), 1047, 2001.
13. H. Kupfer, T. Flügel, F. Richter, P. Schlott, "Intrinsic stress in dielectric thin films for micromechanical components," *Surface and Coatings Technol*, 116-119, 116, 1999.
14. O. Arnon, T.J. Chou, "Wide band measurement of the refractive index of optical thin films during their deposition," *Thin Solid Films*, 91, 23, 1982.
15. S. Venkataraj, R. Drese, Ch. Liesch, O. Kappertz, R. Jayavel, M. Wuttig, "Temperature stability of sputtered niobium-oxide films," *J Appl Phys*, 91 (8), 4863, 2002.
16. C.C. Lee, C.L. Tien, J.C. Hsu, "Internal stress and optical properties of Nb₂O₅ thin films by ion-beam sputtering," *Appl Optics*, 41 (10), 2043, 2002.
17. C. Kittel, *Introduction to Solid State Physics*, 4th ed., Chap 13, John Wiley & Sons, New York (NY), 1971.
18. H.K. Pulker, *Coatings on Glass*, 3rd ed., Chap 8, Elsevier Science Publ. Co. Inc., New York (NY), 1987.
19. H. Leplan, B. Geene, J.Y. Robic, Y. Pauleau, "Residual stresses in silicon dioxide thin films prepared by reactive electron beam evaporation," *J Appl Physics*, 78 (2), 962, 1995.

UCRL-ABS-216582 and ENG-06-0001